Wi-Fi 6 performance measurements of 1024-QAM and DL OFDMA

1st Daan Weller
Security & Network Engineering
University of Amsterdam
Amsterdam, The Netherlands
dweller@os3.nl

2nd Raoul Dijksman Mensenkamp
Security & Network Engineering
University of Amsterdam
Amsterdam, The Netherlands
rdijksman@os3.nl

3rd Arjan van der Vegt
Technology - Connectivity
Liberty Global
Schiphol-Rijk, The Netherlands
avdvegt@libertyglobal.com

4th Jan-Willem van Bloem
Technology - Connectivity
Liberty Global
Schiphol-Rijk, The Netherlands
jvanbloem@libertyglobal.com

5th Cees de Laat
Security & Network Engineering
University of Amsterdam
Amsterdam, The Netherlands
delaat@uva.nl

***Abstract*—IEEE 802.11ax is the new standard introduced by the IEEE that focuses on improving efficiency of Wireless LANs. Among others, two of the newly introduced features are 1024 Quadrature Amplitude Modulation (QAM) and Orthogonal Frequency Division Multiple Access (OFDMA). In this paper, the expected throughput gain of 25% with the new 1024-QAM and expected latency reduction with downlink (DL) OFDMA are examined with state of the art reference boards of two different Wi-Fi chipset manufacturers. Using three Samsung S10 mobile phones as clients, experiments were performed to measure the expected increase in throughput and decrease in latency.**

The 25% increase in throughput with 1024-QAM was achieved, albeit with a maximum range of operation of less than 6 meters when using a maximal transmit power for MCS 11. We observed a very low percentage of packets transmitted using DL OFDMA in the traffic profiles used. We conclude that the introduction of DL OFDMA does not have a significant impact on the latency with the test scenarios covered. The performance of DL OFDMA is heavily dependent on the ability of the access point to properly schedule DL OFDMA transmissions. The number of clients, packet size, and buffer size play an essential role in the scheduling process. Based on our measurements the benefit of DL OFDMA is expected to be limited unless the number of clients is substantially higher than the three clients used, as would be the case in a stadium, train, or mall.

***Index Terms*—Wi-Fi 6, IEEE 802.11ax, DL OFDMA, 1024-QAM**

I. Introduction

The next generation of Wi-Fi is the IEEE 802.11ax standard, also labelled *Wi-Fi 6* by the Wi-Fi Alliance [1][2]. This paper will focus on the added value of two features introduced by IEEE 802.11ax, 1024-QAM, and downlink (DL) OFDMA by answering the following question: What is the performance of 1024-QAM and DL OFDMA of IEEE 802.11ax on 2 state of the art implementations?
The following sub-questions will help answer the main question:

- What is the benefit of introducing 1024-QAM modulation compared to 256-QAM in terms of throughput?
- What is the benefit of the addition of DL OFDMA in terms of latency?

The remainder of this paper is structured as follows: in section II, a literature review of relevant research is given. The methodologies for the experiments are elaborated in section III. Section IV contains the results of the experiments that were conducted. Then we discuss our findings in section V and draw conclusions in section VI. Finally, future work is covered in section VII.

II. Related work

A. Quadrature Amplitude Modulation

Quadrature Amplitude Modulation (QAM) is a technique that is used to modulate (binary) digits to an analogue signal. These signal transmissions are also named *symbols*. Each symbol is transmitted for a certain period, named *symbol time*, and transmissions are separated by *guard intervals*. In IEEE 802.11ax, longer symbol times of $12.8\ \mu s$ and guard intervals ($3.2\ \mu s$, $1.6\ \mu s$ or $0.8\ \mu s$) are introduced. The subcarriers used in IEEE 802.11ax have one quarter of the bandwidth (78.125 KHz) of the subcarriers used in IEEE 802.11ac [3]. Therefore there is a fourfold increase in the number of subcarriers.

The number of bits (b) transmitted is calculated by taking the base 2 logarithmic value of the number of constellation points (P_c): $b = \log_2(P_c)$. Thus, $\log_2 1024 = 10$ bits are modulated in each symbol for 1024-QAM, in contrast to $\log_2 256 = 8$ bits at 256-QAM. Therefore, an increase in throughput of 25% is anticipated for 1024-QAM.

In addition to the modulation, data encoding is used to introduce redundancy to each symbol transmission. For 256-QAM and 1024-QAM, both $3/4$ and $5/6$ encodings can be used as defined in the IEEE 802.11ax draft [1]. In addition, each frame contains a Frame Check Sequence (FCS) to improve error detection.

Theoretical maximum transfer rates can be calculated using the formula defined in the IEEE 802.11 standard [3]:

$$data\ rate = \frac{N_{SD} \cdot R \cdot N_{BPSCS} \cdot N_{SS}}{T_{DFT} + T_{GI}}$$

where N_{SD} is the number of data subcarriers, R is the coding rate, N_{BPSCS} is the number of coded bits per subcarrier per stream, N_{SS} is the number of spatial streams, T_{DFT} is the symbol duration and T_{GI} is the guard interval used.

The Error Vector Magnitude (EVM) metric is widely used throughout the industry to compare transmission quality, expressed in root-mean-square (RMS) or Decibel (dB) values [4]. It provides the magnitude of the error between the ideal signal and the transmitted signal.

In order to plot EVM measurements, EVM values per symbol are needed. To measure the EVM of a single symbol, the summation and averaging can be excluded from the original formula:

$$EVM_{symbol}[dB] = 10\log_{10}\left(\frac{|S_n - S_{0,n}|^2}{|S_{0,n}|^2}\right)$$

The IEEE 802.11ax draft specifies two different requirements regarding the maximum EVM thresholds for 1024-QAM [1]:

- "The relative constellation error shall be less than or equal to -35 dB if amplitude drift compensation is disabled in the test equipment.
- The relative constellation error shall be less than or equal to -35 dB with amplitude drift compensation enabled in the test equipment, and the relative constellation error shall be less than or equal to -32 dB with amplitude drift compensation disabled in the test equipment."

In order to determine the relationship between the EVM measurements and the operational distance from the access point, multiple EVM measurements can be made at different attenuation levels. The resulting EVM values should be lower than the maximum threshold as defined by the IEEE 802.11ax draft and the adjustable attenuation may be converted into an equivalent free-space propagation distance using the Free Space Path Loss (FSPL) model [5].

B. Orthogonal Frequency Division Multiple Access

IEEE 802.11ax introduces Orthogonal Frequency Division Multiple Access (OFDMA) to increase spectral efficiency [2]. OFDMA is the successor to Orthogonal Frequency Division Multiplexing (OFDM) and introduces a new method of transferring data to multiple clients simultaneously using orthogonal subcarriers [6]. This is done by dividing the available subcarriers into the used bandwidth in a number of groups, called *resource units* (RU). Each RU consists of a number of *tones* which indicates the number of subcarriers the RU uses. The number of tones may change to allocate larger or smaller RUs though the transmission time is the same for all RUs in a given transmission.

For each transmission all clients are assigned one of the RUs. This allows for a number of permutations based on the number of clients involved in the transmission and the available RUs. These permutations are defined in the RU allocation table where each permutation has its own index [1].

The RUs are assigned following the RU allocation index. This decision is made by the *scheduler* and depends on the implementation as the IEEE 802.11ax standard does not specify any implementation guidelines. The scheduler makes decisions based on the calculation of transmission times given active flows [6] [7]. Scheduling per transmission depends on link saturation, packet sizes and the number of clients involved in the transmission, among other variables. As OFDMA's purpose is to minimise overhead by sending data to multiple clients simultaneously, a higher number of clients involved in a significant number of transmissions should reveal better latency results.

With OFMDA enabled the maximum throughput of the link is dependent on the RU allocation used. The theoretical maximum throughput is determined by the data rate formula provided earlier with the parameters N_{SS}, R, N_{BPSCS} being replaced by $N_{SS,u}$, R_u, $N_{BPSCS,u}$, respectively, where u stands for the user in question assigned to a given RU [1].

III. Methodology

Our measurements have been performed using two state of the art reference boards of two different vendors. An overview of the setup is presented in Figure 1. The two reference boards were provided in the optimal configuration by the vendors, dating from June 2019. Both reference boards are configured to transmit with a bandwidth of 20 MHz on channel 140 of the 5 GHz spectrum (5.7 GHz). A guard interval of 0.8 μs is used. MIMO is out of scope and disabled; only one spatial stream in the transceiver is enabled.

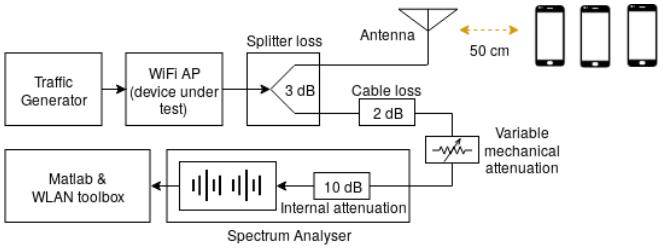

Fig. 1. The general setup used for all experiments. The total conducted pathloss consist of splitter loss (3 dB), cable loss (2 dB), variable mechanical attenuation (20 through 50 dB) and the internal attenuation of the spectrum analyser (10 dB).

The U.FL connector of this radio chain to the antenna is replaced with an U.FL to SMA connector. This connector is connected to an RF splitter with an attenuation of 3 dB. One exit is connected to an antenna, while the other exit is connected to a Rohde & Schwarz FSW67 signal and spectrum analyser via the variable mechanical attenuation. The signal and spectrum analyser is used to make captures of the conducted measurements of the transmitted signal. The total conducted pathloss (CP_{total}) consists of splitter loss (3 dB), cable loss (2 dB), variable mechanical attenuation (20 through 50 dB) and the internal attenuation of the spectrum analyser (10 dB).

Samsung S10 mobile phones equipped with IEEE 802.11ax capable chips (Broadcom BCM4375) are used as stations [8]. These mobile phones are positioned at a distance of 50 cm from the antenna. IxChariot or iPerf were used to generate traffic. The machine running the traffic generator is connected directly by cable to the access point. All experiments performed take place in an RF shielded room. Additionally the spectrum is checked before performing an experiment to make sure the environment is clear of other transmitting devices.

A. 1024-QAM

Throughput measurements are performed using IxChariot UDP throughput profile to a single S10 client. Each measurement runs for a duration of five minutes to one client to measure the average throughput. Throughput values are compared to the theoretical maximum throughput rates. These rates are calculated using the formula as defined by the IEEE 802.11 standard.

Captures of one million samples during 25 ms are made every 30 seconds using the spectrum analyser and Matlab. These captures are afterwards used to calculate the EVM values per symbol in Matlab. OFDMA is disabled for the duration of this experiment as it may dynamically determine the MCS being used to transmit. Four measurements on MCS 11 are made with increasing attenuation from 35 dB to 65 dB with an interval of 10 dB. Increasing the attenuation reduces the signal to noise ratio (SNR) in the received signal and can be mapped to equivalent free space distance using the FSPL model [5]. The FSPL formula can be rewritten to calculate an equivalent distance given a FSPL in dB and frequency:

$$\begin{aligned} FSPL(d,f)[dB] &= 20\log_{10}(d) + 20\log_{10}\left(\frac{4\pi f}{c}\right) \\ \log_{10}(d) &= -\log_{10}\left(\frac{4\pi f}{c}\right) + \frac{FSPL}{20} \\ d(FSPL,f)[m] &= 10^{\left(\frac{FSPL}{20} - \log_{10}(\frac{4\pi f}{c})\right)} \end{aligned}$$

However antennae are used to transmit and receive the signal which has an impact on the FSPL. The formulas may be edited to also include antenna gain and the use of multiple chains:

$$\begin{aligned} G_c[dB] &= G_{tx} + G_{rx} + G_{chains} \\ FSPL(d,f)[dB] &= 20\log_{10}\left(\frac{4\pi df}{c}\right) - G_c \\ d(FSPL,f)[m] &= 10^{\left(\frac{FSPL+G_c}{20} - \log_{10}\left(\frac{4\pi f}{c}\right)\right)} \end{aligned}$$

Using a transmit antenna gain of 4 dBi, a receiver antenna gain of 2 dBi and 4 chains providing 6 dB and the CP_{total} we can determine the distance given one of the configurable attenuation levels. The results of vendor A are used to calculate the distances and as the reference board of vendor A includes a transmission filter, the filter loss (1.5 dB) is included in the calculation. The results of these calculations are given in Table I.

TABLE I
OVERVIEW OF CALCULATED DISTANCE GIVEN TOTAL CONDUCTED PATHLOSS AND ANTENNA GAINS FOR VENDOR A.

$CP_{total}[dB]$	$G_{tx}[dBi]$	G_{rx}	G_{chains}	$distance[m]$
36.5	4	2	6	1.1
46.5				3.5
56.5				11
66.5				35

The attenuation measurements are performed by configuring the reference boards to a transmit power of 18 dBm for each antenna chain[1]. In practice IEEE 802.11ax devices will utilise multiple transmitting chains. This increases the conducted transmit power and thus the EIRP which results in a increased maximum range of operation. For this reason we calculate the distance of operation using four chains, resulting in a conducted transmit power of 24 dBm. As amplitude tracking is enabled on the spectrum analyser the results are compared with an EVM threshold of -35 dB as is defined by the IEEE 802.11ax standard. Lastly, for each attenuation measurement, the ratio of FCS checks are recorded as well. The proportion of successfully decoded Physical Protocol Data Units (PPDU) serves as an indication of the connection quality.

B. DL OFDMA

Latency changes are measured by comparing two experiments for each vendor. Both experiments contain identical set-up and configuration with the exception of the enabling of DL OFDMA. IxChariot or iPerf are used to simulate the traffic profile of a home environment with three stations for a duration of one minute. This profile consists of Voice over IP (VoIP) and Gaming streams to station 1, a video stream to station 2, and a TCP stream to station 3. The VoIP profile consists of a Real-Time Transport (RTP) stream with a 100% activity rate (no silence suppression) and a delay of 20 ms between the voice datagrams. In addition the datagrams are labelled with VoIP Quality of Service (QoS) labels. The video profile also consists of an RTP stream, being a MPEG2 encoded bitstream of 20 Mbps. Datagrams carry seven media frames where each frame is 188 bits. The gaming profile is a custom profile simulating a first-person shooter game. This profile consists of frequently sending and receiving UDP packets with small intervals in milliseconds. For the download profile a high throughput TCP streaming profile is used. This TCP stream is configured to send at maximum speeds with receive and sending buffer sizes of 65,535 bytes.

Captures of one million samples during 25 ms are made every 30 seconds using the spectrum analyser and Matlab. These captures are used to check the DL OFDMA RU allocations and to give an indication of the airtime saturation. The saturation percentage is calculated by dividing the number of samples

[1]In multi-antenna setups, the transmit power is combined for all chains. For example, a setup with four antenna chains with a transmit power of 18 dBm per chain has a conducted transmit power increase of 6 dB, resulting in 24 dBm. The Equivalent Isotropically Radiated Power (EIRP) will then be 28 dBm if antennas with combined antenna gain of 4 dBi are used.

15 dB above the average noise level to the total number of samples.

IV. Results

A. 1024-QAM

The throughput results are presented in Figure 2. The results show throughput values approaching the theoretical maximum for each MCS. Between MCS 8 and 10 a relative increase in throughput of 27% and 29% is achieved for vendor A and B respectively. For MCS 9 and 11 the results show an increase of 26% for vendor A and 27% for vendor B. For clarification the numbers presented are *relative* increases in throughput between the measurements and not the theoretical maximum. In other words the results show that 1024-QAM throughput measurements are closer to the theoretical maximum in comparison to the 256-QAM measurements. Hence the relative increase is larger than 25%.

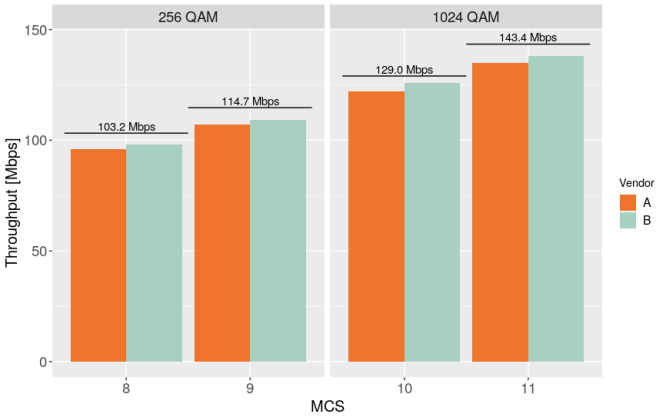

Fig. 2. The average throughput measured for the configured MCS for each vendor. The black lines above the bars indicate the theoretical maximum at which data can be transmitted at the given MCS.

A capture of the constellation diagram at 46.5 dB attenuation with an average EVM of -37.5 dB is presented in Figure 3. As is shown, the symbols are quite clearly distinguishable from each other at this EVM, well below the threshold of -35 dB.

EVM measurements with increasing attenuation are shown in Figure 4. At 35 dB and 45 dB attenuation both vendors produce EVM values significantly under the threshold. From 55 dB and higher both vendors do not produce EVM values under the threshold. However to a certain extent connections may still be successfully maintained with EVMs higher than the threshold. Included in Figure 4 are the measured FCS checks which show binary results; all FCS either pass or fail. Attenuations of 35 dB through 56.5 dB show all FCS checks passed whereas the FCS checks at an attenuation of 65 dB and 66.5 dB all failed. The distance is calculated based on the FSPL model taking into account the internal attenuation of the analyser (10 dB), the antenna gains, 4 transmitting chains, cable loss, splitter loss and the filter loss, resulting in a maximum range of operation of less than 6 meters when using a maximal transmit power for MCS 11.

B. DL OFDMA

We were not able to compare the DL OFDMA results between vendors as vendor B did not have a DL OFDMA scheduler implemented yet. Vendor A dynamically determined whether a transmission is going to be transmitted over DL OFDMA or not. The scheduler made decisions based on multiple variables such as the number of packets in the buffers, the number of clients receiving or sending packets and the size of the packets. At the time of the experiments, the reference board of vendor B forced all transmissions as OFDMA frames when DL OFDMA is enabled. Therefore results were considered individually.

1) Resource Unit Allocation & Spectrum Capture: Vendor A dynamically allocated a RU allocation index for three users as seen in Figure 5 which corresponds to RU allocation index 16. The middle 26 tones within this allocation are not used. This results in 26 tones of the bandwidth being lost, equivalent to a decrease in throughput of 11.1%. In addition, the increased number of subcarriers compared to the IEEE 802.11ac standard is plotted on the y-axis [3].

The reference board provided by vendor B does not yet have the ability to dynamically determine which DL OFDMA allocation index should be used. A fixed allocation index is set for every transmission. However, the implementation only supports a subset of DL OFDMA allocation indices, and this does not include indices for three users. Therefore, allocation index 15 is used, as can be seen in Figure 6. This is an allocation index for five users and is used in every transmission even if no packets are present in the buffers for that user. The other two unused RUs are padded. This resulted in 78 tones of bandwidth lost, corresponding to a decrease of 33.3% of the throughput.

Figure 7 depicts the spectrum view of a DL OFDMA

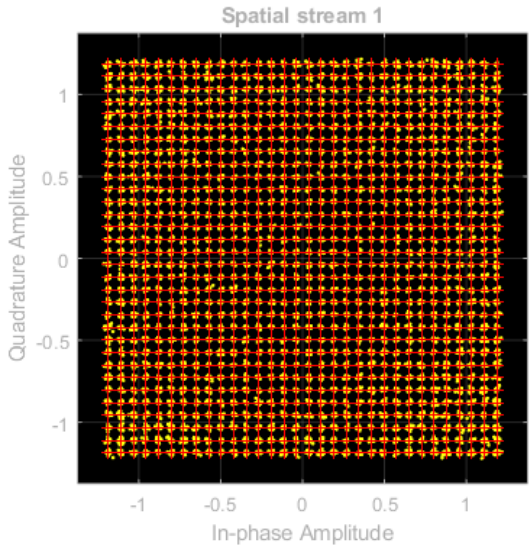

Fig. 3. Constellation diagram of a captured frame transmitted using 1024-QAM modulation at 46.5 dB attenuation, resulting in an average EVM of -37.5 dB.

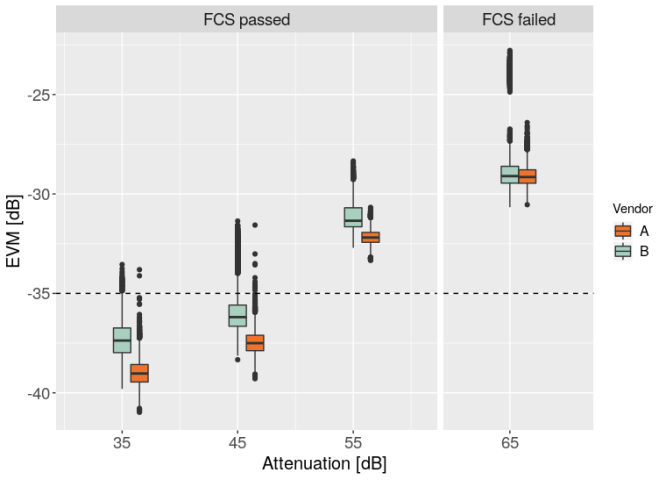

Fig. 4. Boxplot graph of EVM measurements with different attenuation for each vendor. MCS 11 is used, and the EVM threshold is indicated by the dashed line. Included are FCS checks passed for each attenuation used. Calculated distances are presented in Table I.

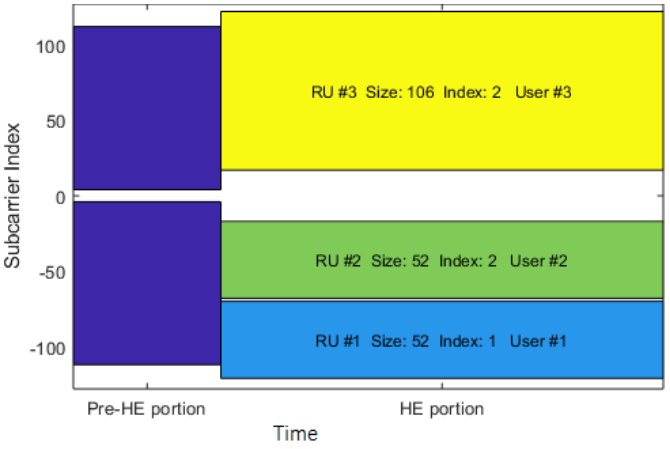

Fig. 5. DL OFDMA RU allocation index 16 dynamically assigned by vendor A.

transmission by the reference board of vendor A. It can be seen that the middle subcarriers are not used in the data transmission, as expected.

2) Airtime Saturation & Latency: First the results of vendor A will be presented. The reference board of vendor A only produced less than 2% DL OFDMA traffic while running the home environment traffic simulation. With DL OFDMA disabled an average throughput of 95 Mbps is achieved. While using DL OFDMA, the average throughput decreased to 75 Mbps. As the percentage of DL OFDMA frames is very low the performance of DL OFDMA in terms of latency remains unclear. The chance of having multiple packets to multiple users at a single moment in time is presumably too low. If the packets are large the scheduler decides it is more efficient not to use DL OFDMA. This might be since 1/9 of the bandwidth is lost while using DL OFDMA as the middle carriers cannot be used with the assigned RU allocation.

Thus the latency difference when introducing DL OFDMA cannot be measured as there is almost no DL OFDMA traffic. Therefore additional experiments have been performed to increase the percentage of DL OFDMA traffic. These experiments required reconfiguration of the used traffic profiles to profiles that are not realistic in the home environment in order to increase the percentage of DL OFDMA traffic.

In order to get a better image of the difference in airtime saturation with DL OFDMA enabled, Iperf [9] was used to create three continuous streams of UDP traffic, one to each client. The streams convey packets of 64 bits at a rate of 1Mbps. Interestingly this traffic configuration produced a near 100% DL OFDMA frames being transmitted. Three captures are made and analysed on the saturation. The results show 27% airtime saturation when DL OFDMA is disabled compared to 30% airtime saturation when DL OFDMA is enabled. Figure 8 depicts the difference in airtime saturation with DL OFDMA on and off. It can be seen that vendor A sends two different frames with DL OFDMA enabled. The first of these frames is the DL OFDMA transmission and is followed by an MU-BLOCK acknowledgement request (MU-BAR). About 8% of the airtime saturation is accounted for by the MU-BARs. As the MU-BAR frames are optional 8% of the airtime saturation can be subtracted. Thus, when the MU-BAR frames are omitted from the airtime saturation this results in a decrease in airtime saturation of $(27 - (30 - 8))/27 \cdot 100 = 18.5\%$ compared to the air time saturation when DL OFDMA is disabled.

The results of vendor B are presented next. Due to the fixed DL OFDMA settings on the reference board of vendor B, all traffic consists of DL OFDMA frames. The throughput decreased from an average of 77 Mbps with DL OFDMA disabled to 11 Mbps with DL OFDMA enabled. This explains why the air-time saturation decreased significantly while DL OFDMA is enabled. We suspect that the implementation of vendor B waits until it has packets to each user in its buffers or until a timeout is hit.

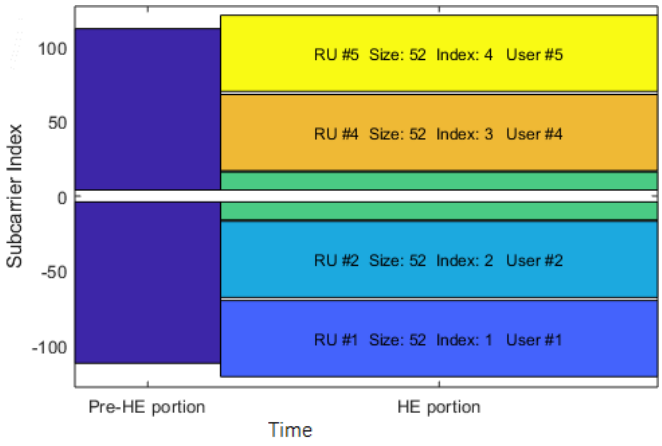

Fig. 6. DL OFDMA RU allocation index 15 used by vendor B. Five resource units are depicted of which three are in use. Note the middle resource unit (green) consisting of two times 13 tones.

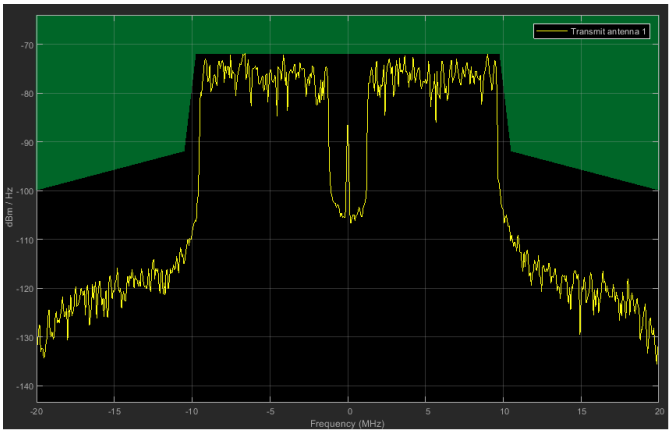

Fig. 7. Spectrum image of the measured DL OFDMA transmission with frequency in MHz on the horizontal and the power in dBm/Hz on the vertical axes.

V. Discussion

As stated in the introduction of FSPL this model assumes an idealised propagation path. The calculated distances should therefore be considered as an indication of the upper limit to the distance over which the signal may propagate for a given decrease in SNR. Thus, the results of Vendor A are used in the calculations as the EVM is lower at higher attenuation, compared to the results of vendor B. However this does not mean that a given MCS is not operable beyond the distance at which EVM measurements are above the threshold. This is indicated by the successful MPDU demodulation ratio. The number of errors in transmissions does increase as the distance between the transmitter and receiver grows. In addition using a lower MCS will increase the range of operation as a more robust coding scheme is used, sacrificing effective throughput.

A transmit power of 18 dBm on a single chain is used while performing EVM measurements. In order to give a better indication of the range of operation using the FSPL model, antenna gains and multiple chains were used in the formula. This increases the EIRP compared to our setup, and thus the effective range of operation used in the calculations. This provides a better indication of the range of operation in practice as implementations will use multiple antenna chains. However these are indications of the best case scenario. In practice results may be significantly worse. The setup used in this paper provides a reference point for future work.

The setup used in the OFDMA experiments consisted of a relatively low number of clients. This is a limiting factor to the exposure of OFDMA traffic as OFDMA is most useful when a much higher number of clients is present, for example in a shopping mall or stadium. In addition only DL OFDMA traffic is considered in this research. During the OFDMA experiments both vendors could not yet combine 1024-QAM with OFDMA. To keep results comparable to non-OFDMA traffic, all traffic was fixed to MCS 9.

VI. Conclusion

The results show a relative throughput increase of 27% and 29% for vendor A and B respectively between MCS 8 and 10. For MCS 9 and 11, the results show an increase of 26% for vendor A and 27% for vendor B. Both vendors show measured throughput close to the theoretical maximum with smaller margins on 1024-QAM. The attenuation measurements show that both vendors are able to produce EVM values below the threshold for 1024-QAM set by the IEEE 802.11ax standard, for attenuation of 35 dB and 45 dB. For 55 dB and 65 dB both vendors produce EVM values above the 1024-QAM EVM threshold. Still both vendors can provide connections up to 55 dB attenuation. At 65 dB attenuation all FCS checks failed for both vendors. The FSPL model is used to calculate the corresponding distance using four transmitting chains with a transmit power of 24 dBm. This results in an upperbound for the operational range of 6 meters as we are working at a maximal transmit power for MCS11.

The current OFDMA scheduler implementation of vendor A does not show downlink (DL) OFDMA to be more efficient while running the home environment traffic simulation. Resource unit (RU) index 16 was used to transmit OFDMA frames to three clients. We speculate that the chance of having small packets to multiple users in the buffers is too low. It seems that the more efficient use of aggregation alleviates the transmission overhead to such a degree that the scheduler does not utilise OFDMA frames. Even when using profiles that increase the number of OFDMA frames being transmitted there is no improvement in latency measured in the used setup with three clients. The implementation of vendor B is restricted to an RU allocation of five users (allocation index 15) which corresponds to a decrease in throughput of 33.3% in the used setup with three clients. This brings the maximum theoretical throughput to 70.6 Mbps. Based on the spectrum captures we speculate that the implementation of vendor B transmits OFDMA frames with fixed sizes and intervals. Due to the high number of lost packets there is a low airtime saturation. We conclude that the latency improvements with the introduction of DL OFDMA highly rely on the scheduler implementation and the number of users. If done incorrectly DL OFDMA can also increase the latency or drastically reduce the throughput. This is in line with our expectations as the benefit of DL OFDMA is expected to be limited unless the number of clients is substantially higher than the three clients used, as would be the case in a stadium, train, or mall.

VII. Future Work

Interestingly the results show similar EVM values for 256-QAM compared to 1024-QAM. This likely results in improved distance of operation using 256-QAM in IEEE 802.11ax as compared to IEEE 802.11ac because of the improved hardware. This is therefore an exciting topic for future work.

While three clients are used to test OFDMA in this research, its benefits will be more apparent in areas where the number of clients is much higher. Studying the effects of having a higher number of users will give more insight into the potential

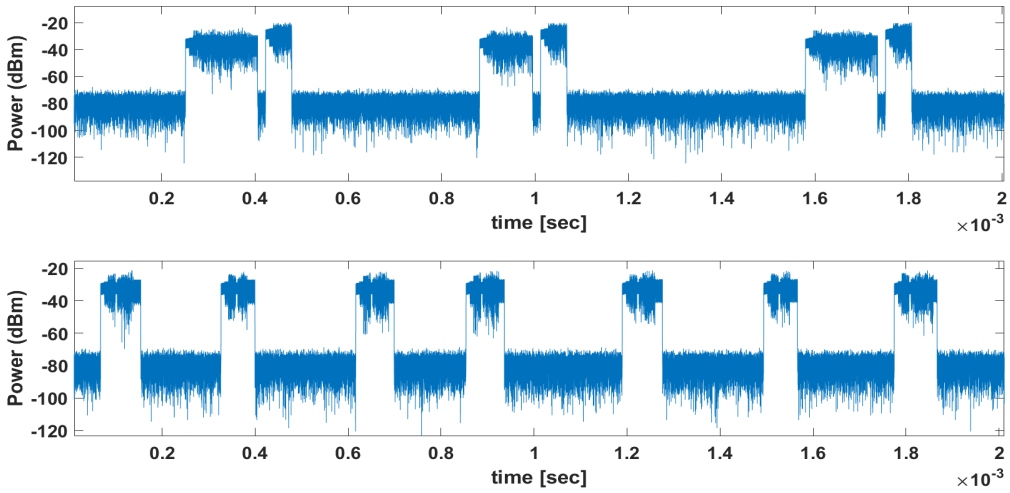

Fig. 8. Airtime saturation comparison with DL OFDMA enabled (top) and DL OFDMA disabled (bottom) of vendor A. Three UDP streams sending 64 bits packets at a rate of 1 Mbps were used to generate the traffic. A near 100% of DL OFDMA frame type of transmission was achieved with this traffic profile. DL OFDMA frames are visible followed by MU-BLOCK ACK requests.

benefits of OFDMA. This research focused on OFDMA with downlink traffic. The theoretical improvement in performance is significant on the uplink channel [10]. Future work on how uplink OFDMA affects the latency in practice is therefore also of interest.

Acknowledgements

This research would not be possible without the reference boards and collaboration from the silicon chipset vendors. We would also like to show our gratitude to MathWorks for collaborating with us during the course of this research.

References

[1] "IEEE Draft Standard for Information Technology – Telecommunications and Information Exchange Between Systems Local and Metropolitan Area Networks – Specific Requirements Part 11: Wireless LAN Medium Access Control (MAC) and Physical Layer (PHY) Specifications Amendment 1: Enhancements for High Efficiency WLAN". In: *IEEE P802.11ax/D4.0, April 2019* (Apr. 2019).

[2] E. Khorov et al. "A Tutorial on IEEE 802.11ax High Efficiency WLANs". In: *IEEE Communications Surveys Tutorials* 21.1 (Mar. 2019), pp. 197–216. ISSN: 1553-877X. DOI: 10.1109/COMST.2018.2871099.

[3] "IEEE Standard for Information technology-Telecommunications and information exchange between systems Local and metropolitan area networks-Specific requirements - Part 11: Wireless LAN Medium Access Control (MAC) and Physical Layer (PHY) Specifications". In: *IEEE Std 802.11-2016 (Revision of IEEE Std 802.11-2012)* (Dec. 2016), pp. 1–3534. DOI: 10.1109/IEEESTD.2016.7786995.

[4] Rishad Ahmed Shafik et al. "On the error vector magnitude as a performance metric and comparative analysis". In: (Jan. 2006). DOI: 10.1109/ICET.2006.335992.

[5] Joseph Shaw. "Radiometry and the Friis transmission equation". In: *American Journal of Physics* 81 (Jan. 2013), pp. 33–37. DOI: 10.1119/1.4755780.

[6] H. Kwon et al. "Generalized CSMA/CA for OFDMA systems: protocol design, throughput analysis, and implementation issues". In: *IEEE Transactions on Wireless Communications* 8.8 (Aug. 2009), pp. 4176–4187. ISSN: 1536-1276. DOI: 10.1109/TWC.2009.080816.

[7] M. Karaca et al. "Resource management for OFDMA based next generation 802.11 WLANs". In: *2016 9th IFIP Wireless and Mobile Networking Conference (WMNC)*. July 2016, pp. 57–64. DOI: 10.1109/WMNC.2016.7543930.

[8] Michelle Alarcon et al. *Samsung Galaxy S10+ Teardown*. 2019. URL: https://www.techinsights.com/blog/samsung-galaxy-s10-teardown.

[9] Jon Dugan et al. *iPerf - The TCP, UDP and SCTP network bandwidth measurement tool*. URL: https://iperf.fr/.

[10] D. Bankov et al. "OFDMA Uplink Scheduling in IEEE 802.11ax Networks". In: *2018 IEEE International Conference on Communications (ICC)*. May 2018, pp. 1–6. DOI: 10.1109/ICC.2018.8422767.